Intercalation Process and Rubber–Filler Interactions of Polybutadiene Rubber/Organoclay Nanocomposites

Chaoying Wan, Wei Dong, Yinxi Zhang, Yong Zhang

School of Chemistry and Chemical Technology, Shanghai Jiao Tong University, Shanghai 200240, People's Republic of China

Received 10 July 2006; accepted 26 June 2007
DOI 10.1002/app.27131
Published online 24 September 2007 in Wiley InterScience (www.interscience.wiley.com).

ABSTRACT: The intercalation process and microstructural development of polybutadiene rubber (BR)/clay nanocomposites cured with sulfur were systematically investigated with respect to the organic modifier (primary and quaternary ammonium compounds) of the clay. X-ray diffraction spectra were recorded at various stages of processing to obtain information about the intercalation process. The rubber–filler interactions was examined on the basis of the surface free energy, stress-softening effect, and crystallization behavior. A well-ordered intercalated structure was obtained in the primary ammonium modified clay (P-OMMT) and quaternary ammonium modified clay (Q-OMMT) filled with BR composite. The BR/Q-OMMT composites showed higher mechanical properties and higher hysteresis under tension and lower crystallization abilities than the BR/P-OMMT composites. The results also show that higher interfacial interactions existed between Q-OMMT and BR than between P-OMMT and BR. © 2007 Wiley Periodicals, Inc. J Appl Polym Sci 107: 650–657, 2008

Key words: fillers; nanolayers; nanotechnology; polybutadiene; rubber

INTRODUCTION

Rubber has been considered an ideal matrix for nanocomposites.[1] The high molecular weight of rubber is beneficial with respect to shearing, which facilitates the peeling apart of the clay layers. The amine compounds used as organophilic intercalants in clays are involved in curing reactions as activators in sulfur-curing rubber systems,[2] which might be energetically favored in exfoliation processes of clay. The formation of rubber/clay nanocomposites depends on several aspects, including the type of intercalant,[3,4] the characteristics of the rubber, the melt-blending conditions, and the vulcanization process.[4,5] Studies on the melt compounding of rubber/clay nanocomposites have involved natural rubber (NR),[4–7] acrylonitrile–butadiene rubber,[8] ethylene–propylene–diene rubber (EPDM),[9,10] and styrene–butadiene rubber.[4] These studies have rarely been related to the formation process of rubber/clay composites and rubber–filler interactions.

Wang et al.[11] prepared intercalated polybutadiene rubber (BR)/clay nanocomposites by direct melt compounding. They found that the intercalation occurred in the compounding process and that the intercalation degree was further enhanced by vulcanization. Wu et al.[4] compared different dispersion conditions of octadecylammonium-modified clay (OC) in NR, styrene–butadiene rubber, and EPDM composites. The mixing process produced intercalated and even exfoliated (NR/OC) structures, whereas the intercalated structure of EPDM/OC occurred mainly during the vulcanization process. Recently, it has been found that clay modified with primary ammonium and quaternary ammonium compounds (DDACs) creates different microstructures in a sulfur-cured polar rubber matrix, such as hydrogenated nitrile rubber[12,13] and epoxidized NR.[14] Deintercalation of the organoclay with a primary amine compound was reported due to a complex amine–dithiocarbamic intermediate formed between the prime amine and the vulcanization accelerator.[10,15–17] Although in the case of quaternary amine compound or dicumyl peroxide curing systems, exfoliated or intercalated structures were obtained. What determines the microstructure of rubber/clay nanocomposites should be investigated. The dependence of the final structure on the compounding or vulcanization process and the interactions between the organic modifier and curing system should also be investigated systematically.

Liao et al.[18] prepared exfoliated BR/clay nanocomposites through *in situ* anionic intercalation polymerization. The molecular weight and trans-1,4-unit of the BR content depended on the intercalant type of clay. Wang et al.[11] prepared intercalated BR/clay nanocomposites via direct melt mixing of BR, sodium clay, and DDAC without the usual pretreatment of the sodium clay; this process was called *in situ* organic modification. The results showed that

Correspondence to: C. Y. Wan (cyw@sjtu.edu.cn).

the tensile strength, elongation at break, and tear strength of the BR/clay/DDAC vulcanizates were greatly improved in comparison with those of the gum BR and BR/pristine clay vulcanizates but were somewhat lower than those of BR/organoclay vulcanizates. The dispersion of clay particles in the BR/clay/DDAC and BR/organoclay composites was much better than that in the BR/pristine clay composite.[19,20] In this study, the effect of organic modifier type and processing condition on the formation of BR/clay nanocomposites were studied. The rubber–filler interactions are discussed in terms of surface energy, stress-softening effect, and crystallization behavior.

EXPERIMENTAL

Materials

The elastomer was a *cis*-1,4-polybutadiene rubber (BR 9000), produced by Shanghai Gaoqiao Petrochemical Corp. (Shanghai, China). It was synthesized by the $Ni(Naph)_2$–$BF_3{\cdot}OEt_2$–$Al(i\text{-}Bu)_3$ catalyst system. The relative amounts of *cis*-1,4-polybutadiene, *trans*-1,4-polybutadiene, and 1,2-polybutadiene structures were 97.3, 1.1, and 1.6 wt %, respectively. The rubber exhibited a Mooney viscosity of ML_{1+4} 100°C = 46. A natural montmorillonite (Na-MMT) and two types of organoclays based on Na-MMT were donated by Zhejiang Fenghong Clay Chemicals Co., Ltd. (Anji, China). The Na-MMT had a cation-exchange capacity of 90 mmol/100 g; two kinds of organoclay were modified, one with octadecyl ammonium chloride [primary ammonium modified clay (P-OMMT)] and one with dimethyl dihydrogenated tallow ammonium chloride [quaternary ammonium modified clay (Q-OMMT)]. The interlayer spacings of the Na-MMT, P-OMMT, and Q-OMMT were 1.22, 2.08, and 3.5 nm, respectively. The interlayer spacing data of the three kinds of clays were obtained via WAXD method. *N*-Cyclohexylbenzothiazole-2-sulfenamide, stearic acid, and zinc oxide (ZnO) were produced by Shanghai Guoyao Chemical Co. (Shanghai, China). Sulfur was produced by Shanghai Gaoqiao Petroleum Co. (Shanghai, China). The molecular structure of BR and the two intercalants for P-OMMT and Q-OMMT were as follows:

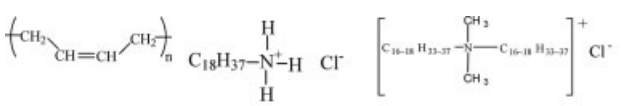

BR | Octadecyl ammonium chloride | Dimethyl dihydrogenated tallow ammonium chloride

Preparation

We made the BR/clay compounds by following three steps. First, BR and 30 phr clay were mixed in an internal mixer (Haake Rheocord 9000, Haake Co., Vreden, Germany) operating at 90°C with a rotor speed of 60 rpm for 6 min. Then, 1.5 phr sulfur, 4 phr ZnO, 2 phr stearic acid, and 2.5 phr *N*-cyclohexylbenzothiazole-2-sulfenamide were added and mixed at 40°C and 60 rpm for another 5 min. Finally, the resultant mixture was compounded further on a two-roll mill at ambient temperature for about 10 min. The obtained compounds were compression-molded under 10 MPa for an optimum cure time to yield vulcanizates.

The addition of 30 phr clay was suggested by previous work of our group[19] devoted to optimizing the mechanical performance of rubber nanocomposites produced by melt compounding.

Characterization

Wide-angle X-ray diffraction (XRD) was used to characterize the clays and the rubber composites. The XRD patterns were obtained with a diffractometer (Dmax-rc, Rigaku, Tokyo, Japan) at a Cu Kα wavelength of 0.1541 nm with a generator voltage of 40 kV and a generator current of 100 mA. The diffractogram was scanned in the 2θ range from 1 to 10° at a rate of 1°/min.

Tensile properties were measured with dumbbell specimens (6 mm wide in the cross-section) according to ASTM D 412-98a. The tear strength was tested according to ASTM D 624-00 with an unnotched 90° angle test piece. Both tensile and tear tests were performed on an Instron IX 4465 tensile machine (Instron Co., Norwood, MA) at a crosshead speed of 500 mm/min. The tensile value represents the average of five specimens, whereas the tear resistance was derived from three parallel tests.

Stress-softening behavior was measured at 500 mm/min on an Instron IX 4465 tensile machine. The samples were stretched to 100% strain followed by a release of stress. Then, the samples were stretched again (second stretching) to the same magnitude of the first stretching. The ratio of the tensile stress at the first and the second stretching at 100% strain [stress retention (R_2)] was calculated. The samples were stretched for a third and fourth time, and the stress retentions (R_3 and R_4) were calculated accordingly. Such sample was placed at room temperature for 24 h before the fifth stretching (R_5). Finally, the sample was stretched for the sixth time after annealing at 70°C for 24 h.

The surface energy and interfacial properties of rubber and clay were studied with Young's equation.[21] The equilibrium contact angles of the solids were measured with a dataphysics OCA20 contact angle instrument (Dataphysics Instrument GmbH, Filderstadt, Germany). Water and diiodomethane were used as testing liquids, and their surface ener-

TABLE I
Surface Energies of Water and Diiodomethane Measured at 20°C[22]

Sample	γ^d (mJ/m^2)	γ^p (mJ/m^2)	γ (mJ/m^2)
Water	21.8	51.0	72.8
Diiodomethane	49.5	1.3	50.8

γ, surface free energy of liquid, γ^d, dispersive component; γ^p, specific component.

gies at 20°C were shown in Table I, which refers to Wu's results.[22]

The crystallization behavior of BR and the BR/clay composites were analyzed with differential scanning calorimetry (DSC; Paris 1, PerkinElmer Co., Norwalk, CT) in a nitrogen atmosphere. Samples of about 10 mg were taken from the rubber compounds. The heating rate was 10°C/min, and the scanning scope was from −60 to 20°C.

RESULTS AND DISCUSSION

Microstructures of the BR/clay composites

Figure 1 shows the XRD patterns of the clays and their BR composites with sulfur used as the curing agent. The developments of the clay interspacings at various stages were recorded and compared. As shown in Figure 1(a), the original characteristic diffraction peak $d(001)$ of Na-MMT was observed at $2\theta = 7.24°$ ($d = 1.22$ nm). When the following three processing stages were compared, small changes in the diffraction peak were observed. The Na-MMT almost kept its original morphology during the compounding process, which meant that the hydrophilic Na-MMT was not compatible with the BR matrix. Figure 1(b) shows that the interspacing of P-OMMT was enlarged from an original 2.08 nm to 2.22 nm after compounding with BR at the first stage, which indicated that partial BR chains intercalated between P-OMMT layers even during this simple blending. The addition of curing additives into the mixer expanded the interspacing to 2.72 nm, which indicated that the curing additives might have adsorbed onto the clay interlayers and expanded the interspacing.[23] A second diffraction peak at a larger angle of 5.65° appeared at the second mixing stage. Furthermore, $d(001)$ moved to a lower angle with increasing intensity after the mixture was compounded on a two-roll mill. The final interspacing of P-OMMT in BR matrix was expanded to 3.5 nm upon vulcanization, and the second peak at 5.52° still existed. The interspacing of P-OMMT was enlarged from 2.08 to 3.5 nm step by step during the compounding and curing process. Figure 1(b) demonstrates that the intercalation of the curing additives and BR chains in P-OMMT layers was a key step occurring in the vulcanization reactions of BR in the clay galleries and resulted in a larger interspacing of the P-OMMT. In sulfur-cured hydrogenated nitrile rubber/clay[12,13] and EPDM/clay[9,10] systems, an addi-

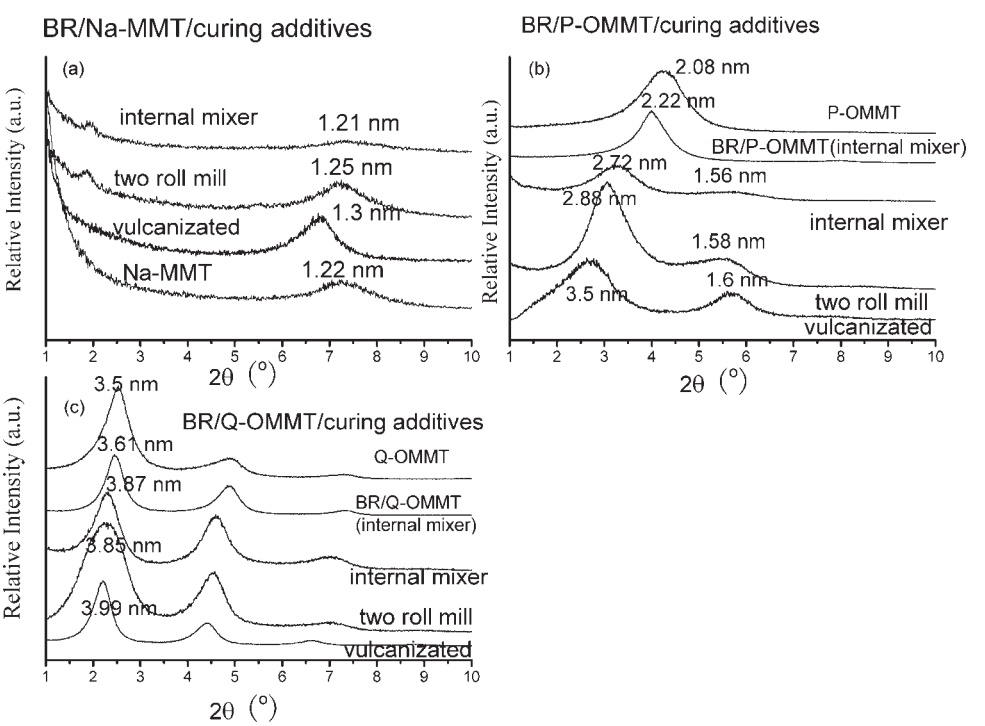

Figure 1 XRD spectra of the clays and BR/clay composites.

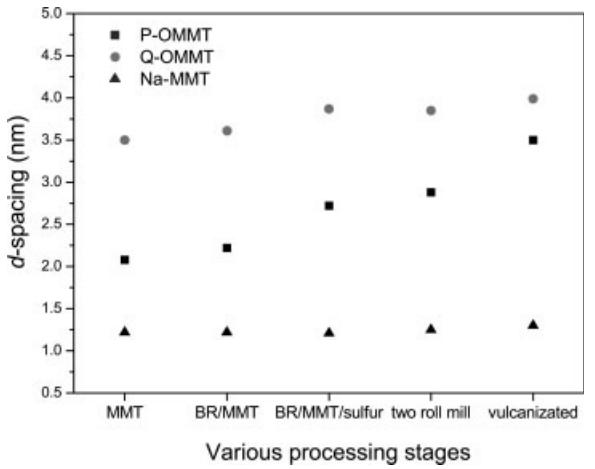

Figure 2 Interspacing data of different clay and BR/clay composites at various processing stages obtained from XRD spectra (MMT = montmorillonite).

tional diffraction peak of clay in the range of $2\theta \approx 5$–7° was attributed by the researchers to clay confinement. Partial primary ammonium intercalants were reported to participate in forming Zn–sulfur–amine complexes. Part or all of the original intercalants were removed out of the clay galleries, which resulted in a collapse of the intercalated structure.[9,10,12,13] Figure 1(b) shows that the second peak at a larger angle began to appear in the compounding process at room temperature and not in the curing process. Also, the position of the second peak at $2\theta = 5.65$–5.52° ($d = 1.56$–1.6 nm) was less related to either the $d(001)$ diffraction peak of P-MMT ($d = 2.08$ nm) or that of Na-MMT ($d = 1.22$ nm). Therefore, this second peak indicated that the intercalation and flocculation of P-OMMT coexisted in the BR matrix.

As shown in Figure 1(c), the Q-OMMT exhibited three diffraction peaks, and the $d(001)$ peak was at 2.52°, which corresponded to a basal spacing of 3.5 nm. The initial interspacing of Q-OMMT was larger than that of P-OMMT because the surfactant, dimethyl dihydrogenated tallow ammonium ions in Q-OMMT had longer molecular chains and a larger volume than octadecyl ammonium ions in P-OMMT. A paraffin-type bilayer was supposed for the intercalant arrangement in Q-OMMT, and a lateral bilayer was supposed for P-OMMT on the basis of the initial interspacing values.[24] The three diffraction peaks of Q-OMMT indicated well-ordered layered structures compared to P-OMMT. Figure 2 shows that the enlargement amplitude of Q-OMMT was lower than that of P-OMMT. This may have been related to the adsorption saturation of the organic molecules within the galleries in the case of the DDACs, but the final interspacing of Q-OMMT was still larger than that of P-OMMT. This means that the initial interspacing of the organoclay was one of the important factors determining its final interspacing in the polymer matrix. As shown in Figure 1(b,c), both BR/P-OMMT and BR/Q-OMMT had well-ordered intercalated structures.

Mechanical properties of the BR/clay vulcanizates

Figure 3 shows the physical and mechanical properties of the BR gum vulcanizates and BR vulcani-

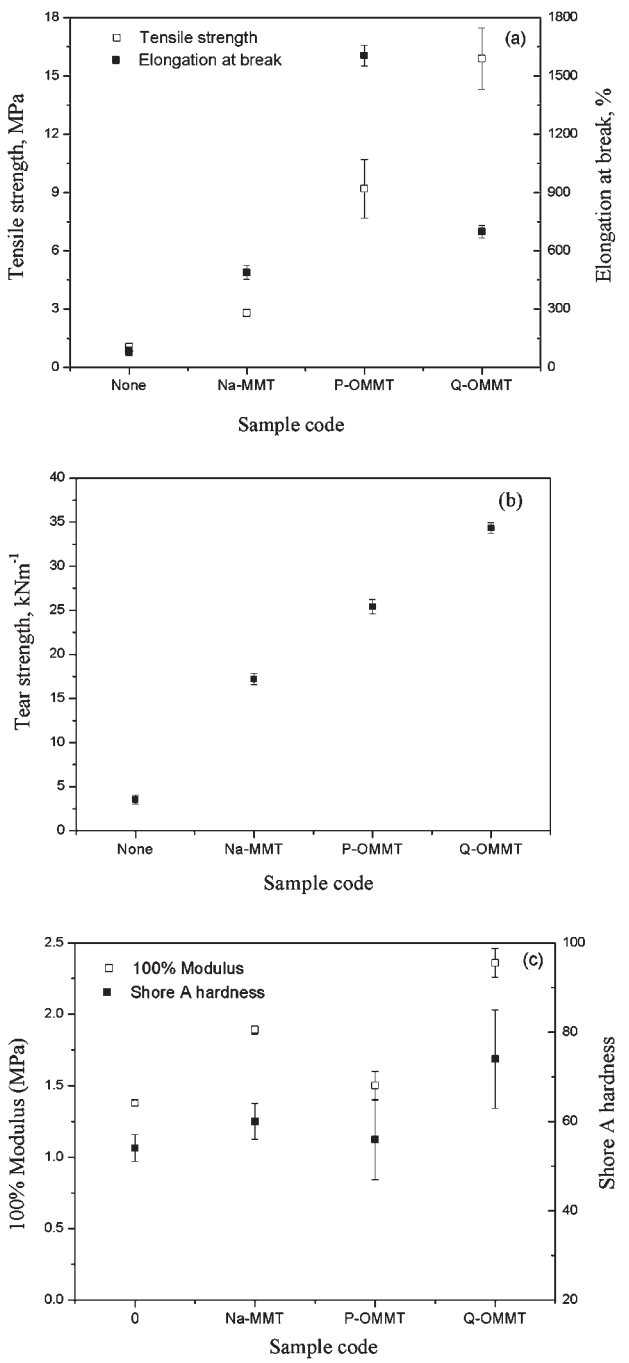

Figure 3 Effect of Na-MMT and different OMMTs on the mechanical properties of the BR vulcanizates.

zates filled with Na-MMT and OMMTs. The OMMT-filled BR vulcanizates showed higher tensile properties and tear strengths than the BR gum vulcanizates and BR/Na-MMT vulcanizates. The Q-OMMT exhibited a higher reinforcement ability than P-OMMT. Compared with the BR gum vulcanizate, the tensile strength and elongation at break of the BR/Q-OMMT vulcanizate were enhanced from 1.04 MPa and 82% to 15.89 MPa and 698%, respectively. The tear strength of BR/Q-OMMT was the highest among the four kinds of vulcanizates and was about 870 and 400% higher than that of the BR gum and BR/Na-MMT vulcanizates, respectively. The 100% modulus and Shore A hardness of the BR/Q-OMMT vulcanizate was the highest among the four kinds of vulcanizates as well. The tensile strength and tear strength of BR/Q-OMMT were comparable to the carbon black and silica-reinforced BR vulcanizate.[3,11,19] P-OMMT and Q-OMMT enhanced the tensile strength and elongation at break of BR simultaneously. The well-ordered intercalated clay layers oriented under the tensile stress, and the BR chains absorbed on the clay layers aligned and slipped along the clay layers. Such a deformation process dissipates much energy, and the strength and elongation at break are consequently enhanced.

Rubber–filler interactions

Bound rubber has been recognized as an important factor in the reinforcement mechanism of rubber and is often considered to be a measure of surface activity.

We found that the Na-MMT and OMMT did not yield any bound rubber with BR, which suggested that Na-MMT/BR or OMMT/BR interactions were very week and were not associated with a chemisorption process.

On the basis of Fowkes' theory,[25] the surface free energy of a solid (γ_s) includes two components, as shown in eq. (1):

$$\gamma_s = \gamma_s^d + \gamma_s^p \tag{1}$$

where γ_s^d is the dispersive component, attributable to London attractions and γ_s^p is the specific (or polar) component, which is due to all other types of polar interactions (e.g., hydrogen bonding and other weakly polar effects).[25,26]

The surface energies of the BR and organoclay were measured by an equilibrium contact angle method and were determined on the basis of the Young–Dupŕe relationship[21]:

$$\frac{(1+\cos\theta)\gamma_l}{2} = \sqrt{\gamma_s^d \gamma_l^d} + \sqrt{\gamma_s^p \gamma_l^p} \tag{2}$$

where θ is the contact angle of liquid on the solid and γ_l^d and γ_l^p are the dispersive and polar components of liquid's surface energy, respectively. The results are shown in Table II.

The interaction energy (γ_{mf}) was measured by eq. (3):

$$\gamma_{mf} = \gamma_m + \gamma_f - 2\sqrt{\gamma_m^d \gamma_f^d} - 2\sqrt{\gamma_m^p \gamma_f^p} \tag{3}$$

where γ_m and γ_f are the surface energies of the BR matrix and clay filler, respectively. γ_m^d and γ_m^p are the dispersive and polar components of matrix's surface energy, and γ_f^d and γ_r^d are the dispersive and polar components of filler's surface energy.

Work of adhesion (W_a) was calculated with eq. (4) according to Owens and Wendt's geometric approach[27]:

$$W_a = \gamma_m + \gamma_f - \gamma_{mf} \tag{4}$$

The equilibrium cohesive work (W_c) is determined by the following equation:

$$W_c = 2\gamma_s \tag{5}$$

The spreading coefficient (S) of rubber on the clay layers was characterized by eq. (5):

$$S = 2(\sqrt{\gamma_m \gamma_f} - \gamma_m) \tag{6}$$

W_a shows the ability of interfacial adhesion and interactions between rubber matrix and fillers. A higher W_a results in a stronger interfacial adhesion and endows positive effects on the mechanical properties of the composites. A smaller γ_{mf} facilitates a good interfacial adhesion, according to eq. (4). Table III shows that the W_a value of BR/P-OMMT was almost equal to that of BR/Q-OMMT, but the γ_{mf} and S values of BR/P-OMMT were higher than

TABLE II
Surface Energies of the Cured BR and Clays

Sample	θ_1 (water)	θ_2 (diiodomethane)	γ_s^d (mJ/m^2)	γ_s^p (mJ/m^2)	γ_s (mJ/m^2)
BR	93.0	47.7	34.6	0.8	35.4
P-OMMT	76.5	48.1	31.3	6.9	38.2
Q-OMMT	80	45.1	31.9	5.2	37.1

TABLE III
Interfacial Properties of the Clay–BR Composites

Sample	W_a (mJ/m^2)	W_c (mJ/m^2)	γ_{mf} (mJ/m^2)	W_a/γ_{mf}	S (mJ/m^2)	Tensile strength (MPa)
BR/P-OMMT	70.5	70.7	3.1	22.5	2.8	9.2
BR/Q-OMMT	70.6	70.7	2.0	34.5	1.8	15.9

those of BR/Q-OMMT. The ratio of W_a and the γ_{mf} value of BR/P-OMMT was lower than that of BR/Q-OMMT, which corresponded to the tensile strength, tear strength, and 100% modulus. Therefore, the value of W_a/γ_{mf} could be used to characterize the rubber–filler interaction.[28]

The stress-softening effect, or Mullins effect, reflecting a kind of viscous loss, can be used to characterize rubber–filler interactions.[29] Figure 4 shows the stress-softening behavior of the BR gum vulcanizate and BR vulcanizates filled with different clays. The four kinds of vulcanizates showed similar stress-softening behavior, in which the BR/Q-OMMT vulcanizate exhibited the highest stress-softening effect. The second tension stress decreased for BR and BR/clay samples compared to the first tension stress, as shown in Figure 4. The stress-softening effect is related to the destruction and reconstruction of crosslinking bonds, local orientation of rubber molecular chains, and interactions between filler and rubber chains.[29] In the process of tension, the intercalated rubber segments or chains might be pulled out of the clay gallery, and the interactions between the rubber and the clay were broken. Such interactions could not be rebuilt quickly at room temperature. That is why the second tension stress of BR and the BR/clay samples was much lower than the first tension stress. The physical adsorption of rubber chains on clay layers is dynamic and can be rebuilt after a long time of relaxation or upon heat treatment. Therefore, in the fifth and sixth stretching stage, the tension stress increased and even exceeded the first tension stress. This phenomenon has not been found in other rubber–filler systems. The exact stress-softening mechanism need to be further studied.

As shown in Table IV, the BR gum vulcanizate and BR/Na-MMT and BR/P-OMMT vulcanizate exhibited similar lower hysteresis compared to BR/Q-OMMT vulcanizate. The Mullins effect of filled vulcanizates reflects the hysteresis of vulcanizates, or the amounts of energy absorbed by the vulcanizates.[30] Therefore, the Q-OMMT filled BR vulcanizate had a higher Mullins effect and indicated a higher reinforcement effect of the Q-OMMT.

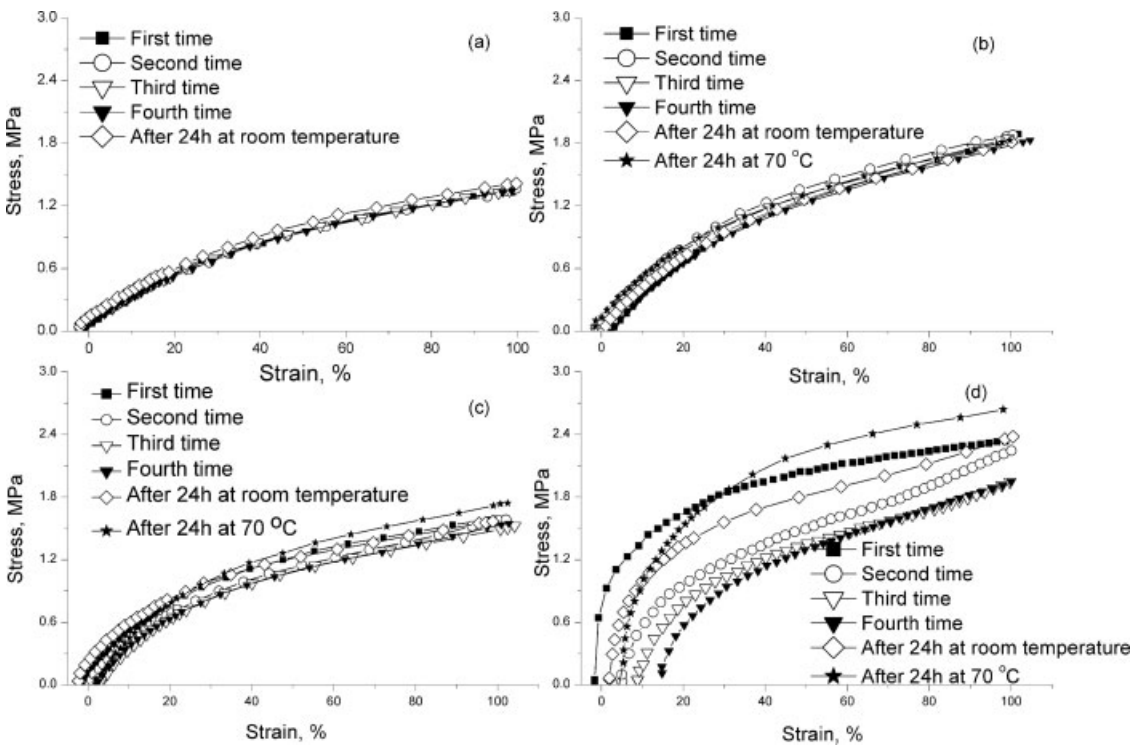

Figure 4 Stress-softening effect of (a) BR vulcanizates and BR vulcanizates filled with (b) Na-MMT, (c) P-OMMT, and (d) Q-OMMT.

TABLE IV
Stress Retention Values of BR and the BR/Clay Vulcanizates During the Stress-Softening Process

	BR	BR/Na-MMT	BR/P-OMMT	BR/Q-OMMT
R_2 (%)	99.88	94.60	95.40	73.22
R_3 (%)	98.93	94.77	93.18	62.64
R_4 (%)	98.46	91.93	92.18	59.26
R_5 (%)	108.57	96.11	99.88	89.49
R_6 (%)	—	100.59	108.57	100.85

The DSC results [Fig. 5 (b) and Table V] showed that the crystalline exothermal peaks of BR/clay composites shifted to a higher temperature compared to that of BR gum, which means that the crystalline growth velocity of BR increased in the presence of clay or that the clay acted as a nucleating agent. In addition, the decreased supercooling degree ($\Delta T = T_m - T_c$, where T_m is the melting temperature and T_c is the crystallization temperature) of BR after the addition of clays also indicated an increase of crystalline growth velocity during the nonisothermal process. However, as shown in Table V, the calculated degree of crystallinity (X_c) of the BR gum decreased compared to those of BR/clay compounds. Increased crystalline growth velocity normally results in an increase in X_c. In the BR/clay compounds, the clays only enhanced the crystalline growth velocity but did not increase the crystalline amount. That might have been due to the interactions between BR and clay layers inhibited BR chain movement so that the final X_c did not increase although the nucleating sites increased. These also resulted in lower T_m values in the three BR/clay compounds than in the BR gum [Fig. 5(a)]. Both T_c and T_m of the BR/P-OMMT compound were higher

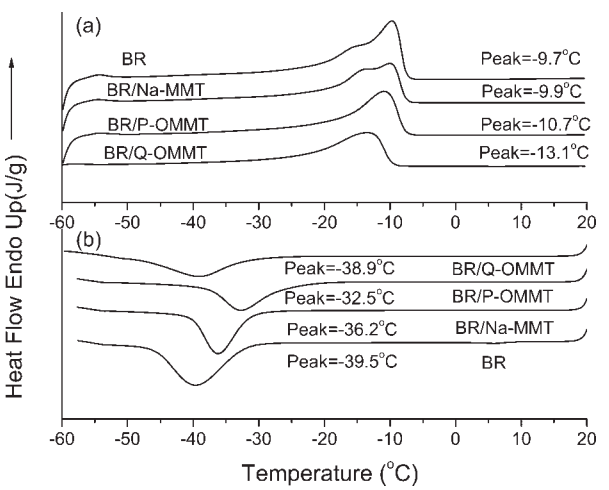

Figure 5 DSC curves of the BR gum and BR/clay compounds.

TABLE V
DSC Results of the BR Gum and BR/Clay Compounds

Sample	T_c (°C)	T_m (°C)	ΔH_c (J/g)	ΔH_m (J/g)	X_c (%)[a]	ΔT (°C)[b]
BR	−39.5	−9.7	34.2	16.6	10.6	29.8
BR/Na-MMT	−36.2	−9.9	23.3	13	8.3	25.5
BR/P-OMMT	−32.5	−10.7	20.2	13	8.3	21.8
BR/Q-OMMT	−38.9	−13.1	18.8	11.1	7.1	25.8

[a] $Xc = \frac{\Delta Hm}{\Delta H_m^0} \times 100\%$, where ΔH_m^0 is the heat of fusion for 100% crystalline BR and $\Delta H_m^0 = 156$ J/g[31] and ΔH_c and ΔH_m are the measured enthalpy of crystallization and enthalpy of fusion for samples.

[b] ΔT is the supercooling degree. $\Delta T = T_m - T_c$.

than those of the BR/Q-OMMT compounds, which means that the crystallization ability of BR was higher in the BR/P-OMMT composites than in BR/Q-OMMT. Because the interfacial interaction of BR/Q-OMMT was stronger than BR/P-OMMT (as shown in Table III), the BR chains were less confined in BR/P-OMMT than in the BR/Q-OMMT composites, and the BR chains were more mobile and could more easily assemble on the clay surface.

CONCLUSIONS

Both octadecylamine P-OMMT and Q-OMMT filled BR cured with sulfur had well-ordered intercalated structures. A second diffraction peak that appeared in the compounding process of BR/P-OMMT indicated homogeneous swelling of P-OMMT and no reaggregation of the layers. The enlargement amplitude of P-OMMT was larger than that of Q-OMMT, although the initial interspacing of P-OMMT was smaller than that of Q-OMMT. Compared with the BR/P-OMMT vulcanizate, BR/Q-OMMT had a higher stress-softening effect and a lower crystallization ability, which were due to stronger interfacial interactions between the BR matrix and Q-OMMT layers. The Q-OMMT effectively reinforced BR compared with P-OMMT and Na-MMT. Consequently, the reinforcement ability of the three kinds of clays was in the order Q-OMMT > P-OMMT > Na-MMT.

References

1. Kocsis, J. K.; Wu, C. M. Polym Eng Sci 2004, 44, 1083.
2. Natural Rubber Science and Technology; Roberts, A. D., Ed.; Oxford University Press: Oxford, 1990.
3. Wang, S. H.; Peng, Z. L.; Zhang, Y.; Zhang, Y. X. Polym Polym Compos 2005, 13, 371.
4. Wu, Y. P.; Ma, Y.; Wang, Y. Q.; Zhang, L. Q. Macromol Mater Eng 2004, 289, 890.
5. López-Manchado, M. A.; Arroyo, M.; Herrero, B.; Biagiotti, J. J Appl Polym Sci 2003, 89, 1.
6. Arroyo, M.; López-Manchado, M. A.; Herrero, B. Polymer 2003, 44, 2447.

7. Joly, S.; Garnaud, G.; Ollitrault, R. Chem Mater 2002, 14, 4202.
8. Nah, C. W.; Ryu, H. J.; Kim, W. D.; Chang, Y. W. Polym Int 2003, 52, 1359.
9. Gatos, K. G.; Thomann, R.; Karger, K. J. Polym Int 2004, 53, 1191.
10. Karger, K. J.; Gatos, K. G. Polymer 2005, 46, 3069.
11. Wang, S. H.; Zhang, Y.; Peng, Z. L.; Zhang, Y. X. J Appl Polym Sci 2005, 98, 227.
12. Konstantinos, G. G.; Nikolaos, S. S.; Anton, A. A.; Ralf, T.; József, K. K. Macromol Mater Eng 2004, 289, 1079.
13. Gatos, K. G.; Szazdi, L.; Pukanszky, B.; Karger, K. J. Macromol Rapid Commun 2005, 26, 915.
14. Varghese, S. Polymer 2003, 44, 3977.
15. Nieuwenhuizen, P. J.; Duin, M. V.; Haasnoot, J. G.; Reedijk, J.; Mcgill, W. J. J Appl Polym Sci 1999, 73, 1247.
16. Nieuwenhuizen, P. J. Appl Catal A 2001, 207, 55.
17. Dirksen, A.; Nieuwenhuizen, P. J.; Hoogenraad, M.; Haasnoot, J. C.; Reedijk, J. J Appl Polym Sci 2001, 79, 1074.
18. Liao, M. Y.; Shan, W.; Zhu, J. D.; Li, Y.; Xu, H. D. J Polym Sci Part B: Polym Phys 2005, 43, 1344.
19. Wang, S. H.; Zhang, Y.; Ren, W. T.; Zhang, Y. X.; Lin, H. F. Polym Test 2005, 24, 766.
20. Wang, S. H.; Zhang, Y.; Peng, Z. L.; Zhang, Y. X. J Appl Polym Sci 2006, 99, 905.
21. Young, T. Philos Trans R Soc London 1805, 95, 65.
22. Wu, S. Polymer Interface and Adhesion; Marcel Dekker: New York, 1982.
23. Zaborski, K. M.; Donnet, J. B. Macromol Symp 2003, 194, 87.
24. Vaia, R. A.; Teukolsky, R. K.; Giannelis, E. P. Chem Mater 1994, 6, 1017.
25. Fowkes, F. M. J Phys Chem 1962, 66, 382.
26. Israelachvili, J. Intermolecular and Surface Forces, 2nd ed.; Academic: London, 1992.
27. Park, S. J.; Brendĺe, M. J. Colloid Interface Sci 1997, 188, 336.
28. Wu, J.; Chen, Y.; Shen, Z. J Mater Sci Lett 1999, 18, 461.
29. Mullins, L. Rubber Chem Technol 1969, 42, 339.
30. Harwood, J. A. C.; Mullins, L.; Payne, A. R. J Appl Polym Sci 1965, 9, 3011.
31. Wunderlich, B. Macromolecular Physics; Academic: New York, 1976; Vol. 1, p 62.